



HAL
open science

On the energy localization in weakly coupled oscillators for electromagnetic vibration energy harvesting

Zakaria Zergoune, Najib Kacem, Nouredine Bouhaddi

► To cite this version:

Zakaria Zergoune, Najib Kacem, Nouredine Bouhaddi. On the energy localization in weakly coupled oscillators for electromagnetic vibration energy harvesting. *Smart Materials and Structures*, 2019, 28 (7), pp.14. <10.1088/1361-665X/ab05f8>. <hal-02472660>

HAL Id: hal-02472660

<https://hal.science/hal-02472660v1>

Submitted on 10 Feb 2020

HAL is a multi-disciplinary open access archive for the deposit and dissemination of scientific research documents, whether they are published or not. The documents may come from teaching and research institutions in France or abroad, or from public or private research centers.

L'archive ouverte pluridisciplinaire HAL, est destinée au dépôt et à la diffusion de documents scientifiques de niveau recherche, publiés ou non, émanant des établissements d'enseignement et de recherche français ou étrangers, des laboratoires publics ou privés.



HAL Authorization

On the energy localization in weakly coupled oscillators for electromagnetic vibration energy harvesting

Zakaria Zergoune, Najib Kacem and Nouredine Bouhaddi

Univ. Bourgogne Franche-Comt, FEMTO-ST Institute,
CNRS/UFC/ENSMM/UTBM, Department of Applied Mechanics, 25000 Besançon,
France

E-mail: zergoune.uni@gmail.com or zakaria.zergoune@femto-st.fr

Abstract. The present paper investigates the implementation of the energy localization phenomenon for enhancing the output harvesting performance. Also in this paper, a linear electromagnetic vibration energy harvester with weakly magnetic coupling is proposed. The designed device is 2 degree-of-freedom (dof) oscillators, which functionalizes the energy localization phenomenon via a spring-magnet array. The proposed concept is made up of moving magnets held by elastic springs and coupled by a repulsive magnetic force with a very low mechanical damping. The energy localization is achieved by mistuning the mass of one of the moving magnets. The experimental and theoretical results showing the benefits of the energy localization phenomenon are reported. The maximal average power density harvested by functionalizing the energy localization is $P_{avg} = 0.8 \mu W.cm^{-3}.g^{-2}.Hz^{-2}$ for a magnetic coupling $\beta = 0.015$.

Keywords: Energy localization, vibration energy harvesting, magnetic coupling, electromagnetism.

1. Introduction

Over the last years, there has been a growing trend towards using wearable, portable devices and embedded systems, such as sensors and other self-sustained electronic systems. However, this growing trend is still limited by the life cycle of their power system which has led to an increasing demand of an alternative of chemical batteries. For this reason, energy harvesting is a promising approach for the next generation of sustainable low-powered portable technologies. Various energy harvesting techniques from different energy sources, available in the environment, have been proposed and designed [1], such as kinetic energy, solar energy, thermal energy, sound energy and so on and so forth. Ambient vibration-based energy harvesters with the ability to convert mechanical vibrations to electrical energy are among these technologies with potential applications for low-powered electronic devices. So far, vibration energy

harvesters **have been** commonly based on four different conversion techniques namely piezoelectricity [2, 3], electromagnetism [4, 5], electrostatics [6] for MEMS technology and magnetostriction [7, 8].

Most of the proposed vibration energy harvesting devices are effectively operating within a limited bandwidth close to their resonance frequency. Therefore, the most important issues concerning the vibration energy harvesters are the improvement of the harvested power density and their frequency bandwidth in which they are effectively operating. Several techniques are discussed to enhance energy harvesting performances, namely the nonlinear and multimodal methods which are widely exposed in order to increase the effective frequency bandwidth and to provide more reliable results [9-16]. Particularly, Many 2 dof vibration harvesters were proposed in the literature with the aim of improving the operating bandwidth. This improvement was achieved by exploiting the advantages of the multimodal approach via the piezoelectric **[17, 18]** or electromagnetic techniques **[19]** or a combination of the both techniques **[20]**.

In regard to the techniques cited above, the present work investigates the benefits of a multimodal method with the functionalization of the energy localization phenomenon for enhancing the harvested power. The approach is implemented using a linear electromagnetic vibration energy harvester with weakly-magnetic coupling. The energy localization phenomenon can be occurred by applying a very small symmetry-breaking perturbation to a periodic structure. This perturbation is manifested in form of a localization and a confinement of the vibrational energy to the perturbed region. This phenomenon was discovered by Anderson [21] in disordered weakly-coupled periodic structures and called Anderson localization. In the field of structural dynamics, quasi-periodic structures are highly sensitive to irregularities and can exhibit mode localization of vibration due to manufacturing and material tolerances. These irregularities lead to dramatic changes in the dynamics of the studied system. Therefore in the structural dynamics field, it has been important to establish criteria capable of predicting the occurrence of the mode localization in order to avoid it in the design stage **[22-24]**.

On the other side, this vibration localization has been used by Spletzer et al. [25] for detecting and identifying an ultrasensitive mass in large arrays of nearly identical microcantilevers with mechanical coupling. Also, Maladji et al. [26] studied this phenomenon on a near periodic system of two pendulums mechanically connected using linear spring. In the present work, the energy localization phenomenon is used as an alternative approach to enhance the harvested power. It is implemented by introducing a perturbation using small masses and coupling array of oscillators via a repulsive magnetic force. The functionalization of the energy localization shows an improvement of 10 % of the harvested power density ($P_{avg} = 0.8 \mu W.cm^{-3}.g^{-2}.Hz^{-2}$) with respect to the case without the

implementation of the energy localization. The used power density metric is adopted with the goal of taking into account the different environmental parameters and the device's size for an efficient comparison [27].

2. Theoretical approach

In this section, two moving magnets are considered in the studied system as illustrated in the equivalent mechanical and electrical model (Figure 1b). The designed harvesting device is modeled using two coupled equations. The canonic equations of motion governing the linear behavior of the designed harvester are expressed as follows:

$$\begin{cases} \ddot{x}_1 + 2\xi\omega_0\dot{x}_1 + \omega_0^2[(1+2\beta)x_1 - \beta x_2] = -\ddot{Y}, \\ \alpha\ddot{x}_2 + 2\alpha\xi\omega_0\dot{x}_2 + \omega_0^2[(1+2\beta)x_2 - \beta x_1] = -\alpha\ddot{Y}, \end{cases} \quad (1)$$

where x_j is the relative displacement of each degree of freedom (dof) with $j = 1, 2$. \ddot{Y} is the basis acceleration of the whole system. $\xi = \xi_e + \xi_m \approx \xi_e$ is the damping factor of the studied system with ξ_e and ξ_m are the electrical and mechanical damping, respectively. The damping factor of the harvesting system is estimated experimentally by the half-power bandwidth method [28]. The mechanical forces are used for guiding the two moving magnets and reducing the mechanical damping factor (Figure 1a). The estimated mechanical damping factor is roughly $\xi_m = 0.11\%$ which can be considered very small compared to the proposed harvesters given in the literature [29, 15] and can be neglected leading to the simplification $\xi \approx \xi_e$. $\alpha = \frac{m_2}{m_1}$ stands for the mistuning coefficient which represents the mass ratio between the perturbed dof oscillator x_2 and the unperturbed dof oscillator x_1 (at $\alpha = 1$, the equivalent masses are $m_1 = m_2 = 6.44 \text{ g}$). $\beta = \frac{k^{mg}}{k_1^{me}}$ is the coupling coefficient with k^{mg} and k_1^{me} are the linear magnetic and mechanical stiffness, respectively. $\omega_0^2 = \frac{k_1^{me}}{m_1}$ is the first resonance frequency. It is assumed that the elastic springs are identical. This assumption leads to the following simplifications $k_1^{me} = k_2^{me} = 137.76 \text{ N.m}^{-1}$.

The natural frequencies ω_1 and ω_2 can then be deduced by conservative system associated to the studied concept and considering the mass mistuning coefficient $\alpha = 1$. Thus, the expressions of the deduced eigenvalues can be written as follows:

$$\begin{cases} \omega_1 = \omega_0 \sqrt{1 + \beta} \approx \omega_0 \left(1 + \frac{\beta}{2}\right), \\ \omega_2 = \omega_0 \sqrt{1 + 3\beta} \approx \omega_0 \left(1 + \frac{3\beta}{2}\right), \end{cases} \quad (2)$$

According to equation (2), the natural frequencies ω_1 and ω_2 are represented by a phenomenon called veering which is characterized by approaching each other as the coupling coefficient $\beta \ll 1$, thereby a weak magnetic coupling between the oscillators should be chosen in order to enhance the efficiency of the energy localization.

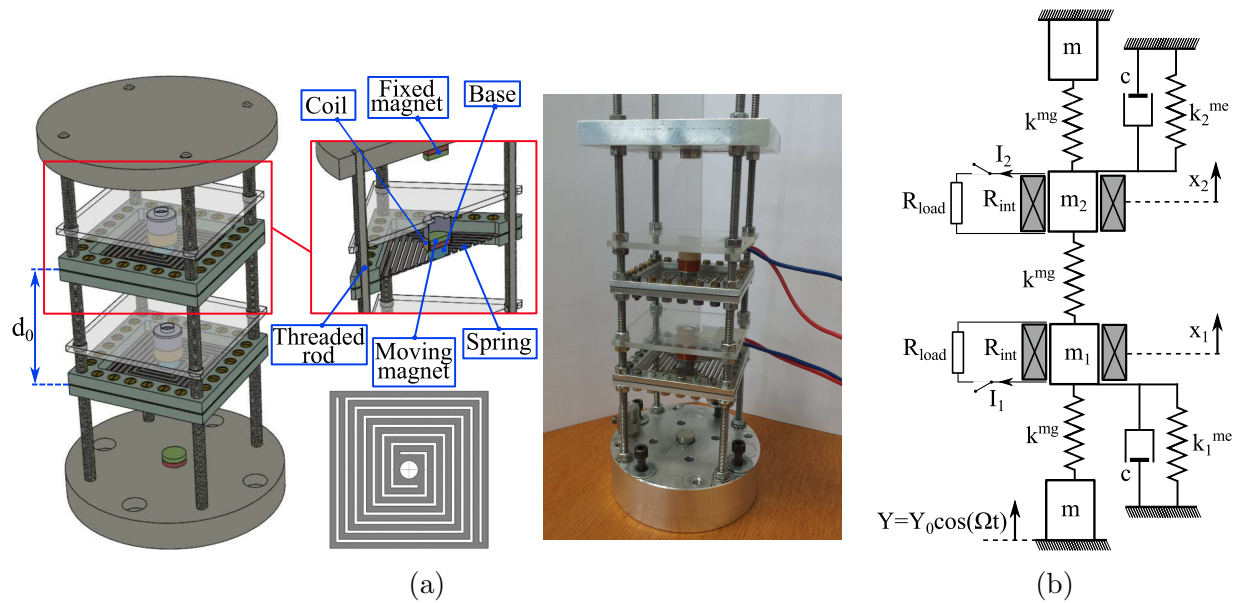


Figure 1: (a) The designed electromagnetic vibration energy harvester (b) the mechanical and electrical equivalent model of the proposed VEH

The repulsive magnetic force between two identical magnets is estimated by a semi-analytical model (equation (3)) proposed by Soares des Santos et al. [30], called the equivalent surface current model (ESC model). The accuracy of this model has been checked by Geisler et al. [31] using Comsol software. The semi-analytic model considers that the magnets are coaxially positioned which is ensured in the present work.

$$F_{ext}^{mg}(d_0) = \mu_0 \pi R^2 M_s^2 \int_0^\infty J_1(\varepsilon R)^2 [2 \cdot \exp(-\varepsilon(d_0 + h_{mag})) - \exp(-\varepsilon \cdot d_0) - \exp(-\varepsilon \cdot (d_0 + 2 \cdot h_{mag}))] \varepsilon^{-1} d\varepsilon, \quad (3)$$

where R , h_{mag} , and M_s are respectively the radius, height and saturation magnetization of the identical magnets and d_0 is the gap between two successive magnets. J_1 stands for the 1st order Bessel function. $\mu_0 = 4\pi 10^{-7} H.m^{-1}$ is the vacuum magnetic Permeability.

The data obtained by the ESC model are fitted for each value of the separate distance d_0 between two successive magnets using a least-squares procedure. The fitted function is expressed as follows:

$$F^{mg}(x) = k^{mg}x + k_3^{mg}x^3, \quad (4)$$

where k^{mg} and k_3^{mg} are respectively the linear and cubic nonlinear magnetic stiffness coefficients. The estimated values of the magnetic linear and nonlinear stiffness coefficients k^{mg} and k_3^{mg} are summarized in Table 1 for different gap values d_0 . By considering the proposed concept, the maximal oscillation amplitude cannot exceed 5 mm. Therefore, the cubic nonlinear stiffness coefficient k_3^{mg} is neglected and only the linear stiffness coefficient k^{mg} is considered through the present work.

Gap d_0 (mm)	40	45	50	55	60	65	70
k^{mg} ($N.m^{-1}$)	5.55	3.34	2.10	1.37	0.93	0.65	0.44
k_3^{mg} ($N.m^{-3}$)	13,740	6,830	3,610	2,010	1,170	620	620
β (%)	4.0	2.4	1.5	1.0	0.7	0.5	0.3

Table 1: Magnetic coupling coefficient β and the corresponding linear and nonlinear magnetic stiffness for different gap values d_0 .

The average of the total harvested power over a single period can be expressed by the following formula [32]:

$$P_{avg} = \left(\frac{\gamma}{\sqrt{2}(R_{load} + R_{int})} \right)^2 R_{load} (\dot{x}_1^2 + \dot{x}_2^2) \quad (5)$$

where γ is the electromagnetic coupling which might be estimated numerically by the following expression [5] :

$$\gamma = 2N\pi R \int \frac{B(x, h_{mag}, R)}{dx} dh, \quad (6)$$

in which $N = 70$ is the number of coil winding and B is the magnetic field calculated by the open software FEMM [33]. The electromagnetic coupling estimated from equation (6) is approximately $\gamma = 1.02 \text{ V.s.m}^{-1}$.

This estimated value is used later to estimate the harvested power.

To quantify the energy localization, the rate τ is calculated by the following expression:

$$\tau(\%) = 100 \frac{|maxV_1 - maxV_2|}{Sup(maxV_1, maxV_2)}, \quad (7)$$

where $maxV_1$ and $maxV_2$ can be either the maximal velocity of the moving magnets for the open-loop circuit or the maximal voltage generated by the two coils for the closed-loop circuit.

Figure 2 exhibits the effect of the energy localization phenomenon on the maximal amplitudes of the both dof by computing its rate τ for a coupling coefficient $\beta = 0.015$. The figure shows that the energy was localized approximately at $\alpha = 1.03$ and 0.95 . It is noticed also that the effect of the energy localization vanishes at a certain mass mistuning coefficient value.

3. Experimental approach

In the current work, the proposed concept uses the energy localization phenomenon for taking advantage of the multimodal approach. This phenomenon is functionalized in the designed system by adding a small mass in order to mistune the spring-magnet array weakly coupled by a repulsive magnetic force. The effect of introducing

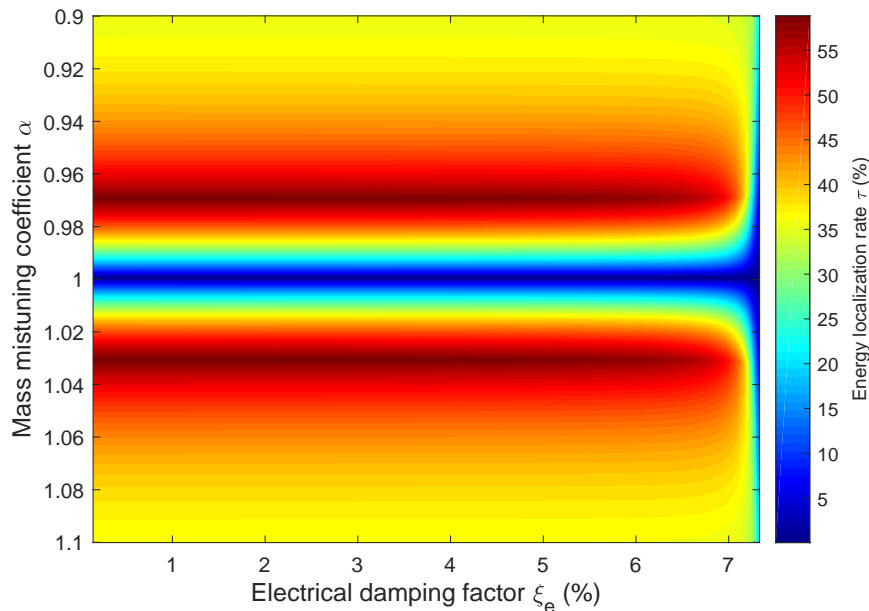


Figure 2: The rate of the energy localization τ as a function of the electrical damping factor ξ_e and the mass mistuning coefficient α .

this phenomenon on the energy harvesting performance is shown experimentally as well. The mechanical and magnetic forces are used for guiding and coupling the center moving magnets as well as reducing the mechanical damping factor (Figure 1a). The designed system is made up of four NdFeB permanent magnets, two fixed magnets placed in the top and bottom of the harvester and two moving magnets held by the springs. The sizes of NdFeB permanent magnets are $h_{mag} = 5 \text{ mm}$ for the height and $R = 6 \text{ mm}$ for the radius. Two bases with 5 mm of height are used between the moving magnets and the springs as shown in Figure 1a to avoid a shock with the coil. The magnets poles have been oriented to repel each other. The coils are placed coaxial with the moving magnets. The magnetic coupling force and the resonance frequency can be tuned by adjusting the gap between the four magnets using the threaded rods.

Figure 3 illustrates the experimental setup used for a sinusoidal excitation. As shown, the designed electromagnetic VEH is mounted on the vibration shaker. A m+p VibPilot monitor and its electronic hardware are used to generate and transmit a sweeping sinusoidal signal with specific output acceleration to the power amplifier of the shaker. This latter supplies mechanical vibrations to the mounted electromagnetic VEH. An accelerometer is mounted on the basis of the VEH device in order to monitor the acceleration \ddot{Y} applied to the prototype. The measured output data (i.e. Voltages, relative velocity and amplitude, and acceleration) are stored by the m+p VibPilot monitor and then treated by Matlab. The frequency during the experiments is swept from 16 Hz to 22 Hz and the acceleration of vibration shaker is set $a_{rms} = 0.008g$ for an open-loop circuit and $a_{rms} = 0.08 \text{ g}$ and 0.1 g in the case

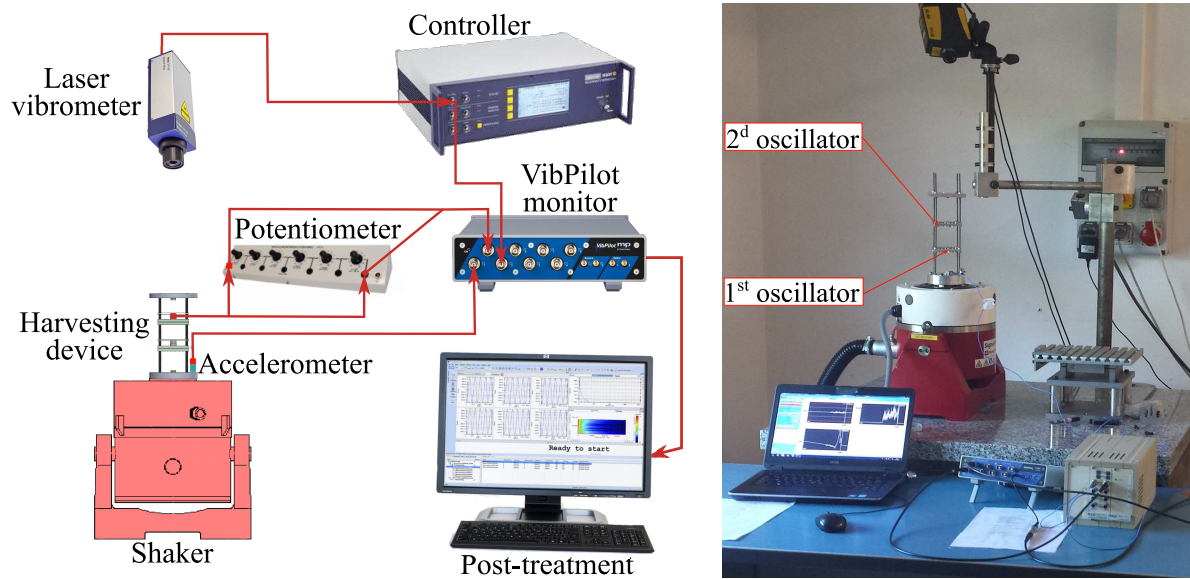


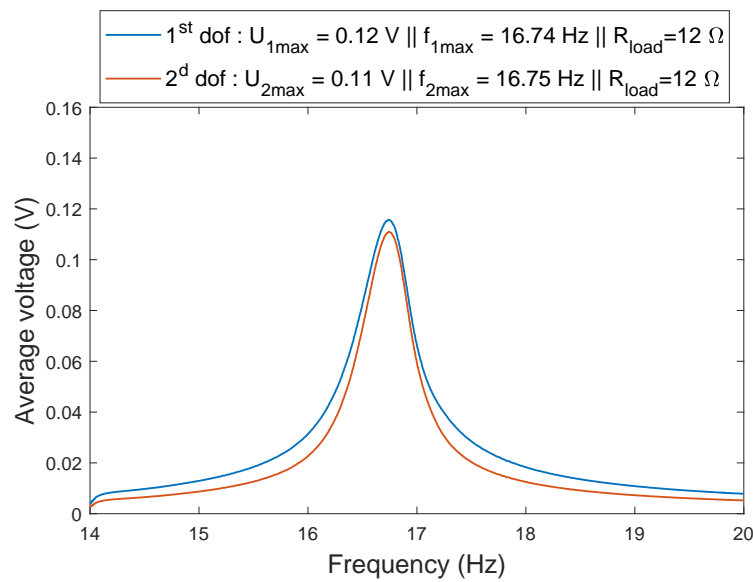
Figure 3: Test bench for a sinusoidal sweep excitation.

of a closed-loop circuit. The laser doppler vibrometer (Polytec OFV-505) is used to measure the velocity of each dof in the open-loop circuit while the output voltage of the coils is stored in the closed-loop circuit. The load resistance, connected to each coil, is controlled using potentiometers.

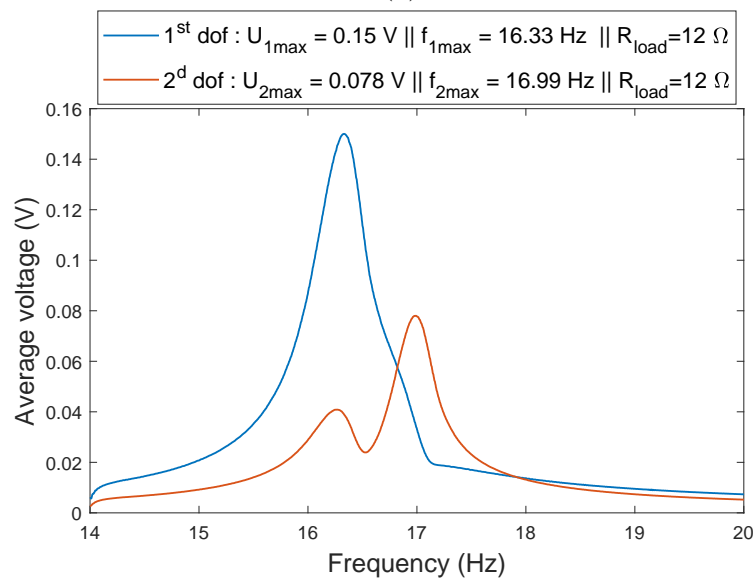
The mass mistuning is achieved by adding small masses ($m_{ad} \approx 0.1 \text{ g}$) is the added mass for each measured point to the first dof oscillator when $\alpha < 1$ or to the second dof oscillator when $\alpha > 1$. The localization test is performed for different magnetic coupling by varying the gap from $d_0 = 40 \text{ mm}$ up to $d_0 = 70 \text{ mm}$ while the resistive load is maintained constant at an optimal value $R_{load} = 12 \Omega$.

Figure 4 shows the experimental results of the designed device for the frequency responses with the basis acceleration $a_{rms} = 0.1 \text{ g}$, a gap $d_0 = 60 \text{ mm}$ and for two cases of the mass mistuning (Figure 4a with $\alpha \approx 1$ and Figure 4b for $\alpha \approx 0.9$). As exhibited in Figures 4b, a perturbation of 7 % of the first dof can lead to a significant variation in the frequency response compared to the reference case $\alpha \approx 1$ (Figure 4). Furthermore, it can be noticed that the frequency broadband is enlarged in Figure 4b compared to the unperturbed case in Figure 4a.

Figure 5 and 6 represent the experimental results performed for the energy localization with sinusoidal excitation. Figure 5 shows the maximum velocity of both dofs at different values of the mistuning coefficient $\alpha = [0.86, 1.3]$ for an open-circuit loop. In the right of the y-axis, it shows the rate of the energy localization at each mistuning coefficient value. The separating distance between the magnets is $d_0 = 60 \text{ mm}$ and the magnetic coupling is consequently $\beta = 0.66 \%$. It is noticed that the small perturbation of one of dofs causes a significant variation of their vibration responses. The rate of the energy localization τ is increased up to 52 % at $\alpha = 1.08$. In addition, it can be observed at $\alpha = 1$ that the designed system does not have the same velocity



(a)



(b)

Figure 4: **Experimental** results of the frequency responses of the proposed VEH **in a closed-loop circuit** with the basis acceleration $a_{rms} = 0.1 \text{ g}$ and the gap $d_0 = 50 \text{ mm}$: (a) $\alpha \approx 1$ and (b) $\alpha \approx 0.9$.

amplitudes because of the stiffness mistuning. This initial mistuning has been caused at the fabrication stage of the springs at which it is too difficult to produce perfect identical samples.

Figure 6 depicts the maximum voltage and the rate of the energy localization of both dofs at different value of the mistuning coefficient $\alpha = [0.85, 1.17]$ for a closed-circuit loop. **It has been noticed, likewise,** that the small perturbation of one of dofs causes a significant variation of their vibration

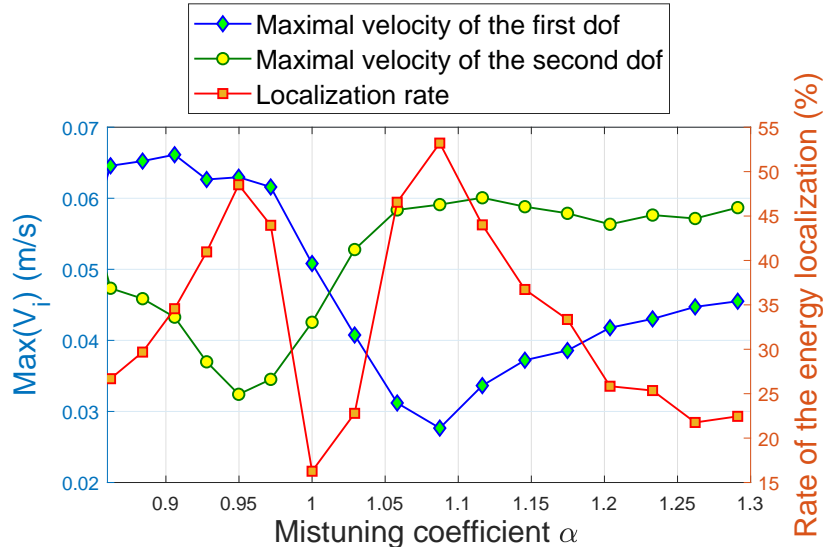


Figure 5: Experimental results of the energy localization for an open-loop circuit with an acceleration $a_{rms} = 0.008 g$ and a gap $d_0 = 60 mm$.

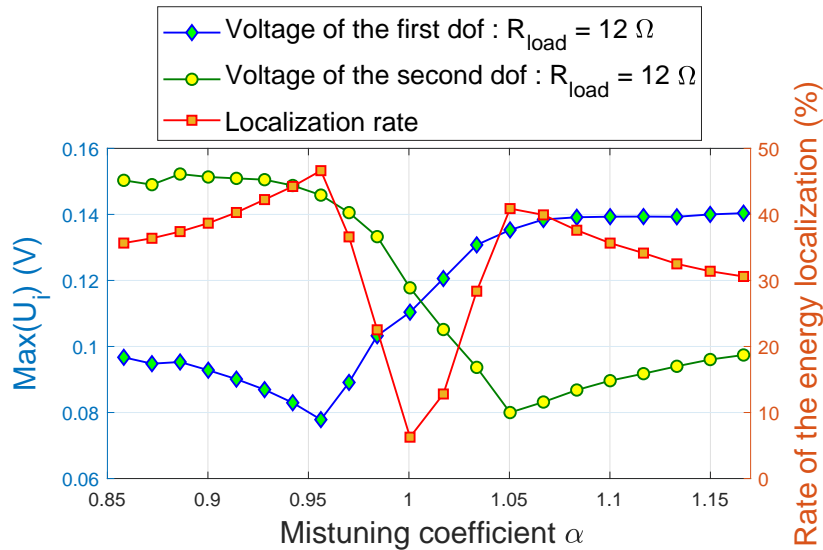


Figure 6: Experimental results of the energy localization for a closed-loop circuit with an acceleration $a_{rms} = 0.1 g$ and a gap $d_0 = 60 mm$.

responses. The rate of the energy localization τ is goes up to 46.63 % at $\alpha = 0.956$.

Whereas, it decreases compared to the open-loop circuit case due to the decreasing of the oscillation amplitude caused by the electrical damping. On the other hand, this later contributes also in the energy harvesting from the designed device and enlarges the effective bandwidth. Therefore, a compromise should be obtained by the implementation of an optimal load resistance.

Figure 7 exhibits the maximal harvested power density at different magnetic coupling values with the resistive load $R_{load} = 12 \Omega$ and the mistuning coefficient

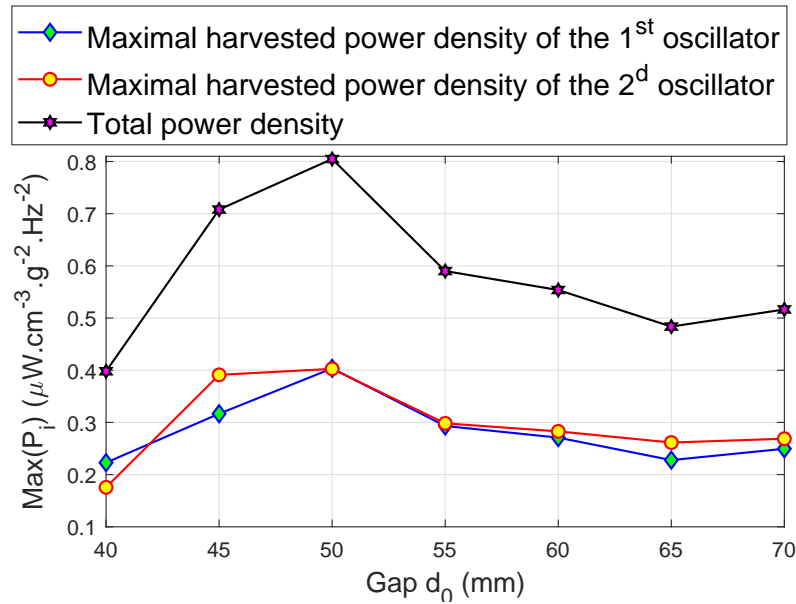


Figure 7: Experimental results of the maximal harvested power density for different gap values with an acceleration $a_{rms} = 0.1 g$ in a closed-loop circuit.

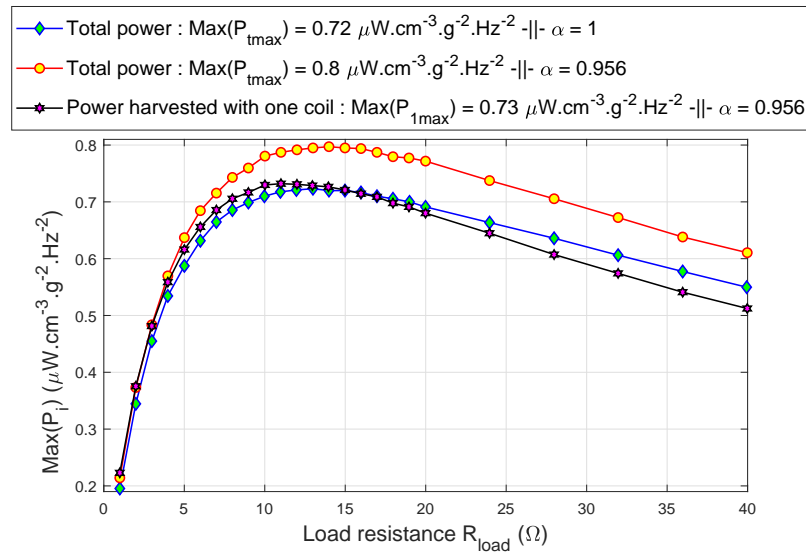


Figure 8: Experimental results of the harvested power at different load resistances for a gap $d_0 = 50 mm$ and an acceleration $a_{rms} = 0.08 g$.

$\alpha = 1$. The magnetic coupling β is controlled by changing the gap d_0 between the successive magnets. As shown in this figure, the magnetic coupling has an effect on the harvested power density. The optimal gap among the measured data is $d_0 = 50 mm$ with a maximal harvested power density $P_{avg} = 0.8 \mu\text{W}\cdot\text{cm}^{-3}\cdot\text{g}^{-2}\cdot\text{Hz}^{-2}$.

The maximal powers at different resistive loads harvested from the designed VEH device in three cases are exhibited in Figure 8 with $\alpha = 0.956$ and 1 and a gap

$d_0 = 50 \text{ mm}$. The magnetic coupling estimated for this gap is roughly $\beta = 0.015$. In the first case, the maximal power is harvested from two coils positioned on the both dof oscillators but without any mass perturbation ($\alpha \approx 1$) while in the second case the maximal power is harvested from two coils with a mistuning coefficient $\alpha = 0.956$. On the other hand, the third case represents the maximal power harvested only from one coil positioned on the perturbed dof oscillator with a mistuning coefficient $\alpha = 0.956$. As shown in this Figure remarkably, there is an increase of approximately 10 % of the maximal harvested power in the second case with $\alpha = 0.956$ compared to the one in the first case with $\alpha \approx 1$. This improvement has been achieved thanks to the energy localization implemented by mistuning the first dof oscillator. Whilst the maximal power scavenged in the first and third cases are roughly identical.

4. Conclusion

In this paper, a linear multimodal electromagnetic VEH with weakly-magnetic coupling **is proposed** in order to scavenge efficiently the ambient vibration energy by functionalizing the energy localization phenomenon. The elastic spring structure, used in the designed VEH device, permits to reduce significantly the mechanical damping factor $\xi_m = 0.11 \%$ compared to existing VEH devices [15, 29, 34, 35]. **The paper shows** that the energy localization phenomenon allows enhancing the harvested performance of the perturbed system by approximately 10 % compared to the non-perturbed system with a mass mistuning coefficient $\alpha \approx 0.956$. In addition, this functionalization permits harvesting the ambient vibration energy efficiently from **one coil instead of two coils positioned only on the perturbed dof oscillator**. Thus, the number of the used wires and coils can be reduced while keeping an identical performance and then avoid the phase problem. Also, it permits simplifying the electronic part, which shall be in charge of rectifying and storing the obtained signal. Finally, the proposed concept can be generalized to a large-scale quasi-periodic system and the device's size can be reduced in order to improve more the harvested power density. Furthermore, the neglected cubic geometric non-linearity can be considered and combine it with the implementation of the energy localization in order to enlarge the effective bandwidth and enhance the harvesting power of the proposed device.

Acknowledgments

This work has been supported by the EIPHI Graduate School (contract "ANR-17-EURE-0002")

5. References

- [1] C. Wei and X. Jing, "A comprehensive review on vibration energy harvesting: Modelling and realization," *Renewable and Sustainable Energy Reviews*, vol. 74, pp. 1–18, 2017.

- [2] A. Toprak and O. Tigli, "Piezoelectric energy harvesting: State-of-the-art and challenges," *Applied Physics Reviews*, vol. 1, p. 031104, 2014.
- [3] S. Priya, H.-C. Song, Y. Zhou, R. Varghese, A. Chopra, S.-G. Kim, I. Kanno, L. Wu, D. S. Ha, J. Ryu, and R. G. Polcawich, "A review on piezoelectric energy harvesting: Materials, methods, and circuits," *Energy Harvesting and Systems*, vol. 4, pp. 3–39, 2017.
- [4] Z. Wu, J. Tang, X. Zhang, and Z. Yu, "An energy harvesting bracelet," *Applied Physics Letters*, vol. 111, p. 013903, 2017.
- [5] S. Dirk and M. Yiannos, *Electromagnetic Vibration Energy Harvesting Devices*. Springer, 2012.
- [6] Y. Zhang, T. Wang, A. Zhang, Z. Peng, D. Luo, R. Chen, and F. Wang, "Electrostatic energy harvesting device with dual resonant structure for wideband random vibration sources at low frequency," *Review of Scientific Instruments*, vol. 87, p. 125001, 2016.
- [7] Z. Yang, K. Nakajima, R. Onodera, T. Tayama, D. Chiba, and F. Narita, "Magnetostrictive clad steel plates for high-performance vibration energy harvesting," *Applied Physics Letters*, vol. 112, p. 073902, 2018.
- [8] L. Wang and F. G. Yuan, "Vibration energy harvesting by magnetostrictive material," *Smart Materials and Structures*, vol. 17, p. 045009, 2008.
- [9] S. Mahmoudi, N. Kacem, and N. Bouhaddi, "Enhancement of the performance of a hybrid nonlinear vibration energy harvester based on piezoelectric and electromagnetic transductions," *Smart Materials and Structures*, vol. 23, no. 7, pp. 75–24, 2014.
- [10] N. Tran, M. H. Ghayesh, and M. Arjomandi, "Ambient vibration energy harvesters: A review on nonlinear techniques for performance enhancement," *International Journal of Engineering Science*, vol. 127, pp. 162–185, 2018.
- [11] R. M. Toyabur, M. Salauddin, H. Cho, and J. Y. Park, "A multimodal hybrid energy harvester based on piezoelectric-electromagnetic mechanisms for low-frequency ambient vibrations," *Energy Conversion and Management*, vol. 168, pp. 454–466, 2018.
- [12] I. Abed, N. Kacem, N. Bouhaddi, and M. L. Bouazizi, "Multi-modal vibration energy harvesting approach based on nonlinear oscillator arrays under magnetic levitation," *Smart Materials and Structures*, vol. 25, no. 2, pp. 25–18, 2016.
- [13] C. Drezet, N. Kacem, and N. Bouhaddi, "Design of a nonlinear energy harvester based on high static low dynamic stiffness for low frequency random vibrations," *Sensors and Actuators A: Physical*, vol. 283, pp. 54–64, 2018.
- [14] J. Cao, S. Zhou, W. Wang, and J. Lin, "Influence of potential well depth on nonlinear tristable energy harvesting," *Applied Physics Letters*, vol. 106, p. 173903, 2015.
- [15] P. V. Malaji and S. F. Ali, "Magneto-mechanically coupled electromagnetic harvesters for broadband energy harvesting," *Applied Physics Letters*, vol. 111, p. 083901, 2017.
- [16] H. Deng, Y. Du, Z. Wang, J. Zhang, M. Ma, and X. Zhong, "A multimodal and multidirectional vibrational energy harvester using a double-branched beam," *Applied Physics Letters*, vol. 112, p. 213901, 2018.
- [17] L. Zhao, L. Tang, and Y. Yang, "Enhanced piezoelectric galloping energy harvesting using 2 degree-of-freedom cut-out cantilever with magnetic interaction," *Japanese Journal of Applied Physics*, vol. 53, p. 060302, 2014.
- [18] A. A. A. Zayed, S. F. M. Assal, and A. M. R. F. El-Bab, "Wide bandwidth nonlinear 2-dof energy harvester: Modeling and parameters selection," *IEEE International Conference on Multisensor Fusion and Integration for Intelligent Systems (MFI), Daegu*, pp. 97–102, 2017.
- [19] S. G. Burrow and L. Penrose, "A 2 dof vibration harvester for broadband and multifrequency harvesting using a single electro-magnetic transducer," *Journal of Physics: Conference Series*, vol. 557, p. 012031, 2014.
- [20] H. y. Wang, L. h. Tang, Y. Guo, X. b. Shan, and T. Xie, "A 2dof hybrid energy harvester based on combined piezoelectric and electromagnetic conversion mechanisms," *Journal of Zhejiang University SCIENCE A*, vol. 15, pp. 711–722, 2014.
- [21] P. W. Anderson, "Absence of diffusion in certain random lattices," *Physical Review Journals*

- Archive*, vol. 109, p. 1492, 1958.
- [22] C. Pierre, D. M. Tang, and E. H. Dowell, “Localized vibrations of disordered multispan beams: Theory and experiment,” *AIAA Journal*, vol. 25, pp. 1249–1257, 1987.
 - [23] C. Pierre and E. H. Dowell, “Localization of vibrations by structural irregularity,” *Journal of Sound and Vibration*, vol. 114, pp. 549–564, 1987.
 - [24] C. Pierre, “Weak and strong vibration localization in disordered structures: A statistical investigation,” *Journal of Sound and Vibration*, vol. 139, pp. 111–132, 1990.
 - [25] M. Spletzer, A. Raman, H. Sumali, and J. P. Sullivan, “Highly sensitive mass detection and identification using vibration localization in coupled microcantilever arrays,” *Applied Physics Letters*, vol. 92, p. 114102, 2008.
 - [26] P. V. Malaji and S. F. Ali, “Energy harvesting from near periodic structures,” *Vibration Engineering and Technology of Machinery*, vol. 23, pp. 411–420, 2014.
 - [27] S. D. Moss, O. R. Payne, G. A. Hart, and C. Ung, “Scaling and power density metrics of electromagnetic vibration energy harvesting devices,” *Smart Materials and Structures*, vol. 24, p. 023001, 2015.
 - [28] J.-T. Wang, F. Jin, and C.-H. Zhang, “Estimation error of the half-power bandwidth method in identifying damping for multi-dof systems,” *Soil Dynamics and Earthquake Engineering*, vol. 39, pp. 138–142, 2012.
 - [29] B. P. Mann and N. D. Sims, “Energy harvesting from the nonlinear oscillations of magnetic levitation,” *Journal of Sound and Vibration*, vol. 319, no. 1-2, pp. 515–530, 2009.
 - [30] M. P. Soares dos Santos, J. A. F. Ferreira, J. A. O. Simoes, R. Pascoal, J. Torrao, X. Xue, and E. P. Furlani, “Magnetic levitation-based electromagnetic energy harvesting: a semi-analytical non-linear model for energy transduction,” *Scientific Reports*, vol. 6, no. 18579, 2016.
 - [31] M. Geisler, S. Boisseau, M. Perez, P. Gasnier, J. Willemin, I. Ait-Ali, and S. Perraud, “Human-motion energy harvester for autonomous body area sensors,” *Smart Materials and Structures*, vol. 26, no. 3, p. 035028, 2017.
 - [32] N. G. Stephen, “On energy harvesting from ambient vibration,” *Journal of Sound and Vibration*, vol. 293, pp. 409–425, 2006.
 - [33] D. C. Meeker, “Finite element method magnetics,” <http://www.femm.inf>, 2006.
 - [34] W. Wang, J. Cao, N. Zhang, J. Lin, and W.-H. Liao, “Magnetic-spring based energy harvesting from human motions: Design, modeling and experiments,” *Energy Conversion and Management*, vol. 132, pp. 189–197, 2017.
 - [35] C. Saha, T. ODonnell, N. Wang, and P. McCloskey, “Electromagnetic generator for harvesting energy from human motion,” *Sensors and Actuators A*, vol. 147, pp. 248–253, 2008.